Surface-enhanced Raman scattering and biophysics

2002 J. Phys.: Condens. Matter 14 R597

(http://iopscience.iop.org/0953-8984/14/18/202)

INSTITUTE OF PHYSICS PUBLISHING JOURNAL OF PHYSICS: CONDENSED MATTER

J. Phys.: Condens. Matter **14** (2002) R597–R624 PII: S0953-8984(02)21355-7

TOPICAL REVIEW

Surface-enhanced Raman scattering and biophysics

Katrin Kneipp[1], **Harald Kneipp, Irving Itzkan, Ramachandra R Dasari and Michael S Feld**

Physics Department, Technical University Berlin, D 10623 Berlin, Germany
and
G R Harrison Spectroscopy Laboratory, Massachusetts Institute of Technology, Cambridge, MA 02139, USA

E-mail: kneipp@usa.net

Received 13 December 2001, in final form 5 April 2002
Published 26 April 2002
Online at stacks.iop.org/JPhysCM/14/R597

Abstract

Surface-enhanced Raman scattering (SERS) is a spectroscopic technique which combines modern laser spectroscopy with the exciting optical properties of metallic nanostructures, resulting in strongly increased Raman signals when molecules are attached to nanometre-sized gold and silver structures. The effect provides the structural information content of Raman spectroscopy together with ultrasensitive detection limits, allowing Raman spectroscopy of single molecules. Since SERS takes place in the local fields of metallic nanostructures, the lateral resolution of the technique is determined by the confinement of the local fields, which can be two orders of magnitude better than the diffraction limit. Moreover, SERS is an analytical technique, which can give information on surface and interface processes.

SERS opens up exciting opportunities in the field of biophysical and biomedical spectroscopy, where it provides ultrasensitive detection and characterization of biophysically/biomedically relevant molecules and processes as well as a vibrational spectroscopy with extremely high spatial resolution.

The article briefly introduces the SERS effect and reviews contemporary SERS studies in biophysics/biochemistry and in life sciences. Potential and limitations of the technique are briefly discussed.

Contents

[1] Author to whom any correspondence should be addressed.

1. Introduction

Laser spectroscopic methods play an increasingly important role in biophysics/biochemistry and in life sciences. Application of spectroscopy includes both the field of basic research in biophysics/biochemistry and the development of new methods for diagnosis of disease and therapy control. Identification and structural characterization, including monitoring structural changes of molecules, play a central role in biophysical/biochemical spectroscopy. Therefore, vibrational spectroscopic techniques such as Raman spectroscopy, which provide high structural information content, are of particular interest.

A great disadvantage in any application of Raman spectroscopy results from the extremely small cross section of the Raman process, which is 12–14 orders of magnitude below fluorescence cross sections. Therefore, in the 1970s, a discovery which showed unexpectedly high Raman signals from pyridine on a rough silver electrode attracted considerable attention [1], particularly after experiments in different laboratories gave evidence that the enormously strong Raman signal must be caused by a true enhancement of the Raman scattering (RS) efficiency itself and not by more scattering molecules [2, 3]. Within the next few years, strongly enhanced Raman signals were verified for many different molecules [4] which had been attached to various 'rough' metal surfaces, and the effect was named 'surface-enhanced Raman scattering (SERS)'. For an overview see [5, 6]. The discovery showed promise to overcome the traditionally low sensitivity problem in Raman spectroscopy.

Estimated enhancement factors of the Raman signal started with modest factors of 10^3–10^5 in the first reports on SERS. Later, many authors claimed enhancement factors of about 10^{10}–10^{11} for dye molecules in surface-enhanced resonance Raman (SERRS) experiments [7–13].

About 20 years after the discovery of the effect, new methods for determining cross sections effective in SERS resulted in unexpectedly large cross sections on the order of at least 10^{-16} cm^2/molecule corresponding to enhancement factors of about 14 orders of magnitude compared with 'normal' non-resonant RS [14]. Such effective Raman cross sections, on the same order of magnitude as fluorescence cross sections of 'good' laser dyes, made RS a single-molecule tool [15–23].

Another generally interesting aspect of SERS is attributed to its spatial resolution. Exploiting local optical fields of special metallic nanostructures, SERS can provide lateral resolutions better than 10 nm [24–27], which is two orders of magnitude below the diffraction limit and even smaller than the resolution of common near field microscope tips.

Since its early days, the SERS effect has also been particularly appealing in the field of biophysics and biochemistry for several reasons.

Most exciting for biophysical studies might be the trace analytical capabilities of the SERS effect together with its high structural selectivity and the opportunity to measure Raman spectra from extremely small volumes. Particularly, single-molecule capabilities open up exciting

perspectives for SERS as a tool in laboratory medicine and for basic research in biophysics, where SERS can offer interesting new aspects compared with fluorescence, which is widely used as a single-molecule spectroscopy tool in biophysics. One of the most spectacular applications of single-molecule SERS might appear in the field of rapid DNA sequencing using the Raman spectroscopic characterization of specific DNA fragments down to structurally sensitive detection of single bases without the use of fluorescent or radioactive labels [18].

Interesting aspects in biophysical applications of SERS come also from exploiting SERRS. In addition to the increased cross sections, resonance Raman scattering (RRS) has the advantage of higher specificity, since the resonance Raman spectrum is dominated by molecular vibrations which are related to the part of the molecule responsible for the appropriate resonant electronic transition. SERRS opens interesting opportunities for large biomolecules, where it allows a selective vibrational probe of the chromophoric systems such as chlorophyll, pheophytin and carotenoids [28–33]. As a further advantage, the fluorescence background, which can make RRS spectroscopy extremely difficult, has been quenched in many SERRS experiments by new nonradiative decay channels provided by the SERS-active metal.

Another useful capability of SERS in the field of biophysics comes from the potential of the method for providing information on molecules residing on surfaces and on surface and interface processes. For example, 'SERS-active' silver or gold electrodes with a defined potential can be used as a model environment for studying biologically relevant processes, such as charge transfer transitions in cytochrome c [34, 35].

There are excellent reviews that summarize SERS studies on biological molecules in the 1980s and early 1990s [36–41]. Therefore, this article will mainly review SERS studies in biophysics and life sciences performed within the last half decade.

After introducing today's understanding of the SERS effect, we review contemporary SERS studies in that field. The potential and limitations of SERS in biophysics/biochemistry and in life sciences as a tool in biophysical and biomedical spectroscopy are considered.

2. Raman scattering and surface-enhanced Raman scattering

Before discussing the effect of SERS, we briefly recall the Raman effect [42, 43]. In the 'photon picture', we consider the Raman effect as a scattering process between a photon and a molecule (see also figure 1(a)). Incident photons $h\nu_L$ are inelastically scattered from a molecule and shifted in frequency by the energy of its characteristic molecular vibrations $h\nu_M$. Frequency-shifted scattered photons can occur at lower and higher energy relative to the incoming photons, depending on whether they interacted with a molecule in the vibrational ground state or an excited vibrational state. In the first case, photons lose energy by exciting a vibration and the scattered light appears at a lower frequency ν_S, called the Stokes scattering. By interacting with a molecule in an excited vibrational state, the photons gain energy from the molecular vibrations and the scattered signal appears at higher frequency ν_{aS}, called anti-Stokes scattering.

In a 'classical view' of the Raman effect, light is an electromagnetic wave which induces a dipole moment in the molecule. The generation of this dipole moment by the incoming electric field is modulated by the molecular vibrations, since the polarizibility α is a function of the vibrational coordinate Q. Therefore, the induced dipole oscillates not only at the frequency of the incoming field, but also at 'side bands' at the sum and difference frequencies between the incoming light and the molecular vibrations. This results in the appearance of Stokes and anti-Stokes'side bands' in the reradiated light.

Figure 1(b) shows the schematics of fluorescence and RS in a molecular energy level diagram together with typical fluorescence and Raman spectra. In many cases, fluorescence

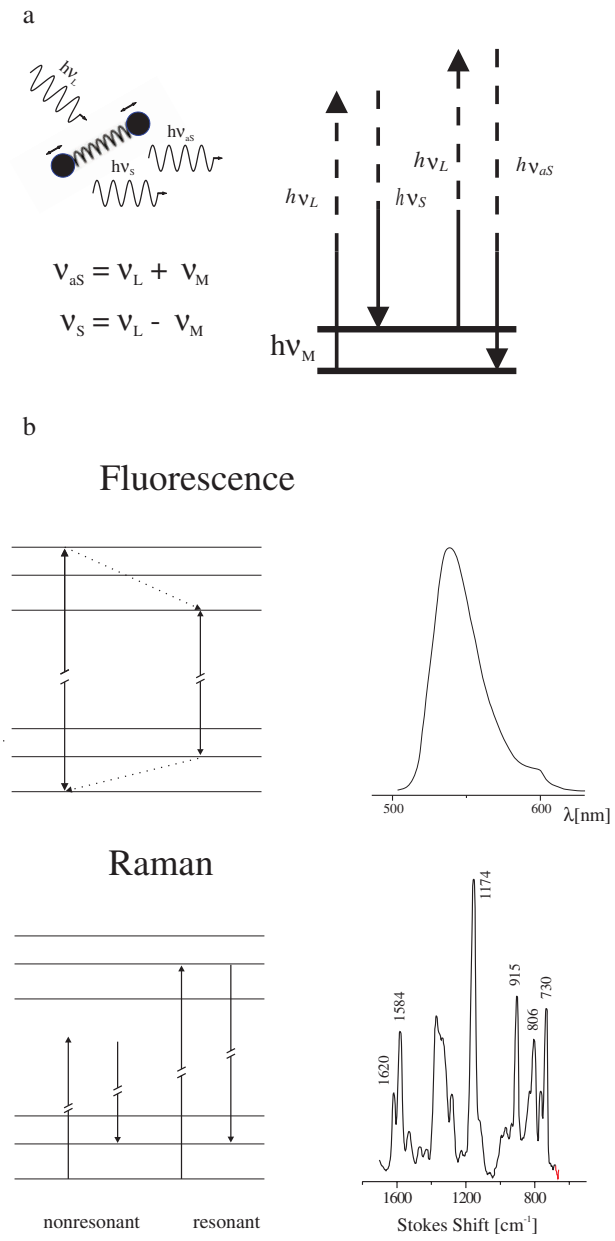

Figure 1. (a), (b) Schematic diagrams of RS and fluorescence.

spectra are relatively 'broad bands' and do not provide so much structural information on the molecule. The Raman effect probes vibrational levels of the molecule, which depend on the kinds of atom and their bond strengths and arrangements in a specific molecule. Therefore, a Raman spectrum provides a structural 'fingerprint' of a molecule.

Note that in nonresonant RS excitation and/or scattered photons are not in resonance with any real molecular transition. The interaction with the molecule is not due to an absorption

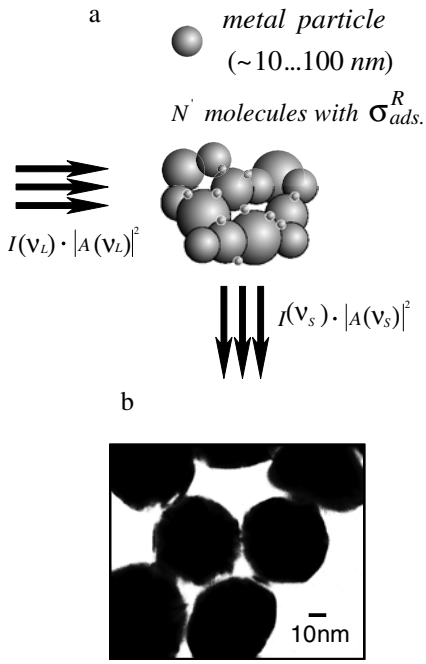

Figure 2. Schematic diagram of SERS: molecules (small spheres) are attached to an aggregate of spherical metal colloidal particles (a). For comparison, see the electron microscopic view of a cluster of colloidal gold particles (b).

and emission process, but due to scattering. This is also the case for so-called RRS, when the excitation laser frequency is in resonance with electronic transitions. In the case of RRS, the RS process becomes stronger, but it is still a different and much weaker process compared with fluorescence. Raman cross sections are between 10^{-31} and 10^{-29} cm^2/molecule; the larger values occur only for resonant RS. Fluorescence cross sections are determined by the product of the absorption cross section and fluorescence quantum yield. They can reach 10^{-16} cm^2/molecule.

In SERS molecules are attached to a metallic 'nanostructure'. The effect was discovered from pyridine adsorbed on electrochemically roughened silver electrodes [1–3]. In 1979 enhanced RS signals from pyridine had also been measured in aqueous silver and gold colloidal solutions. These experiments showed that SERS is not so much a 'surface effect' as it is a 'nanostructure effect' and provided the first clear experimental demonstration of the important role of surface plasmon resonances in SERS [44].

Figure 2(a) shows a schematic diagram of a SERS experiment [19]. The 'nanostructure' is an aggregate of spherical metal colloidal particles; for comparison, see the electron micrograph of colloidal gold particles in figure 2(b).

In 'normal' RS, the total Stokes Raman signal $P^{\mathrm{RS}}(\nu_S)$ is proportional to the Raman cross section σ^R_{free}, the excitation laser intensity $I(\nu_L)$ and the number of molecules in the probed volume N.

$$P^{\mathrm{RS}}(\nu_S) = N\sigma^R_{\mathrm{free}} I(\nu_L). \tag{1}$$

To estimate the SERS Stokes power $P^{\mathrm{SERS}}(\nu_S)$, formula (1) has to be modified in order to describe the specific effect(s) of the metal nanostructures. From the very early days of SERS

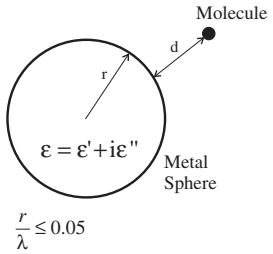

$$E_M = E_0 + E_{sp}$$

E : field of a point dipole in the center of the sphere

$$E_{sp} = r^3 \frac{\varepsilon - \varepsilon_0}{\varepsilon + 2\varepsilon_0} E_0 \frac{1}{(r+d)^3}$$

Figure 3. Simple schematic diagram for understanding the concept of electromagnetic SERS enhancement (for an explanation see the text).

there were experimental observations indicating that there might not exist only one 'SERS mechanism' and that different effects might contribute to the observed enhanced Raman signal. In principle, two effects might be operative in a SERS experiment and are considered in formula (2):

(i) the scattering takes place in the enhanced local optical fields of the metallic nanostructures (electromagnetic field enhancement) and
(ii) a molecule in contact with a metal (nanostructure) exhibits a 'new Raman process' at a cross section larger than the Raman cross section of a free molecule (chemical or electronic enhancement, first-layer effect).

$$P^{\mathrm{SERS}}(\nu_s) = N' \sigma^R_{\mathrm{ads}} |A(\nu_L)|^2 |A(\nu_S)|^2 I(\nu_L). \tag{2}$$

In formula (2), $A(\nu_L)$ and $A(\nu_S)$ express enhancement factors for the laser and for the Raman-scattered field, respectively. σ^R_{ads} describes an (increased) cross section of the new Raman process of the adsorbed molecule. N' is the number of molecules which are involved in the SERS process and can be smaller than the number of molecules in the probed volume N.

Some ideas on the origin of the electromagnetic field enhancement factors $A(\nu)$ and the increase of σ^R_{ads} compared with σ^R_{free} are discussed in the next section.

2.1. SERS mechanisms and SERS enhancement factors

Figure 3 shows a simplified schematic diagram for understanding the concept of electromagnetic SERS enhancement. The metallic 'nanostructure' is a small sphere with the complex dielectric constant $\varepsilon(\nu)$ in a surrounding medium with a dielectric constant ε_0. The diameter of the sphere ($2r$) is small compared with the wavelength of light (Rayleigh limit).

A molecule in the vicinity of the sphere (distance d) is exposed to a field E_M, which is the superposition of the incoming field E_0 and the field of a dipole E_{sp} induced in the metal sphere. The field enhancement factor $A(\nu)$ is the ratio of the field at the position of the molecule and the incoming field

$$A(\nu) = \frac{E_M(\nu)}{E_0(\nu)} \sim \frac{\varepsilon - \varepsilon_0}{\varepsilon + 2\varepsilon_0} \left(\frac{r}{r+d} \right)^3. \tag{3}$$

$A(\nu)$ is particularly strong when the real part of $\varepsilon(\nu)$ is equal to $-2\varepsilon_0$. Additionally, for a strong electromagnetic enhancement, the imaginary part of the dielectric constant needs to be small. This conditions describe the resonant excitation of surface plasmons of the metal sphere.

In an analogous fashion to the laser field, the scattered Stokes or anti-Stokes field will be enhanced if it is in resonance with the surface plasmons of the metal sphere. Taking into account enhancing effects for the laser and the Stokes field, the electromagnetic enhancement factor for the Stokes signal power $G(\nu_S)$ can be written as

$$G_{em}(\nu_S) = |A(\nu_L)|^2 |A(\nu_S)|^2 \sim \left| \frac{\varepsilon(\nu_L) - \varepsilon_0}{\varepsilon(\nu_L) + 2\varepsilon_0} \right|^2 \left| \frac{\varepsilon(\nu_S) - \varepsilon_0}{\varepsilon(\nu_S) + 2\varepsilon_0} \right|^2 \left(\frac{r}{r+d} \right)^{12}. \quad (4)$$

This formula based on a very simple model already describes important properties and peculiarities of the electromagnetic SERS enhancement. It shows that the enhancement scales as the fourth power of the local field of the metallic nanostructure and that it is particularly strong when excitation *and* scattered fields are in resonance with the surface plasmons. This is automatically the case for low-frequency Raman modes and explains that the scattering powers of different Raman bands in a spectrum fall off with increasing vibrational energy. Electromagnetic SERS enhancement does not require direct contact between molecule and metal but it strongly decreases with growing distance described by the decay of the field of a dipole over the distance $[1/d]^3$ to the fourth power, resulting in $[1/d]^{12}$.

Maximum values for electromagnetic enhancement for isolated single colloidal silver and gold spheroids are on the order of 10^6–10^7 [45–47]. Theory predicts stronger enhancement of electromagnetic fields for sharp features and large curvature regions, which may exist on silver and gold nanostructures. For example, it was shown that the electromagnetic SERS enhancement factor can be increased up to nearly 10^{11} when the sphere degenerates and becomes 'sharper' at one edge [48]. Also, closely spaced interacting particles can provide extra field enhancement [49]. Electromagnetic enhancement factors up to 10^{11} have been estimated for the midpoint between two silver or gold spherical particles separated by a gap of 1 nm near the gap sites between two particles in proximity [48].

In many experiments, SERS-active substrates consist of a collection of silver or gold nanoparticles exhibiting fractal properties, such as colloidal clusters formed by aggregation of colloidal particles or metal island films [18, 50–52]. Figure 4 shows SERS-active colloidal silver particles in different aggregation stages. A comparison between the electron microscope view and the light microscope view shows strong similarities and demonstrates the fractal nature of these structures. In such colloidal cluster structures, the individual dipole oscillators of the small isolated particles couple, thereby generating normal modes of plasmon excitation that embrace the cluster and cover a wide frequency region from the visible to the near infrared (NIR) [25, 53–55]. The broadening of the plasmon resonance when colloidal clusters are formed is demonstrated in figure 4, which shows the relatively narrow absorption spectrum of isolated silver colloidal particles centred at about 420 nm together with the broad extinction curve for silver colloidal clusters ranging from about 400 to 1000 nm. The excitation is not distributed uniformly over the entire cluster but tends to be spatially localized in so-called 'hot' areas [25, 56]. Therefore, the surface of a fractal colloidal cluster structure shows a very inhomogeneous field distribution. Figure 5 illustrates the inhomogeneous field distribution on a silver cluster [57]. This theoretical result was confirmed by near field measurements [58–60]. The size of the 'hot areas' can be as small as a few nanometres [26, 27]. Their locations depend strongly on the geometry of the fractal object and on the excitation wavelength and polarization of the optical fields. Particularly strong field enhancement for colloidal silver and gold clusters should exist in the NIR wavelength range. The strongly confined 'hot spots' provide the opportunity to select single nano-objects spectroscopically within a larger population [27] or to probe selectively parts of large molecules. When optical excitation is localized in such small 'hot spots', extremely large electromagnetic SERS enhancement (proportional to field enhancement to the fourth power!) up to 10^{12} was theoretically predicted for these areas. The

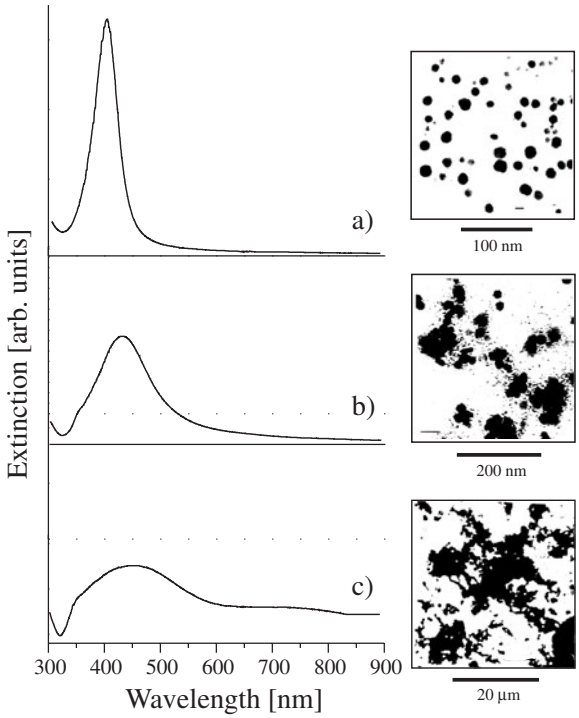

Figure 4. SERS-active colloidal silver particles in different aggregation stages, demonstrating the fractal nature of these structures together with the appropriate extinction curves.

order of magnitude of the enhancement factor has been confirmed in single-molecule SERS experiments, where the 'normal' Raman signal of 10^{14} methanol molecules appears at the same level as the surface-enhanced Raman signal of a single molecule [15, 18]. In those experiments on colloidal silver and gold clusters, total nonresonant SERS enhancement factors on the order of 10^{14} have been observed, which can be understood by a superposition of a factor 10^{12} electromagnetic SERS enhancement and a factor 100 chemical enhancement. Electromagnetic enhancement factors approaching 10^{12} corresponding to field enhancement factors on the order of 10^3 has been also confirmed by surface-enhanced nonlinear RS, where signals nonlinearly depend on the enhanced local fields. The electromagnetic enhancement factors for Stokes, pumped anti-Stokes and hyper-RS experiments scale as theoretically predicted from the appropriate nonlinear process [61, 62].

All the experimental findings described above give compelling evidence for an electromagnetic field enhancement. If SERS were just an electromagnetic field enhancement effect, a strong SERS signal should exist for each molecule in the close enough vicinity of a silver or gold nanostructure. On the other hand, experimental observations such as dependence of the effect on the chemical nature of the molecule and a strong molecular selectivity provide clear indications for the existence of an (additional) 'chemical' SERS enhancement. For example, methanol does not show any SERS enhancement. Other experimental observations which hint at mechanism(s) other than electromagnetic field enhancement include SERS enhancement measured from molecules on metal surfaces, which are 'flat' on the nanometre scale, as well as the dependence of the enhancement factor on the electrode potential. Moreover, best electromagnetic SERS enhancement factors leave a gap of about two orders of magnitude

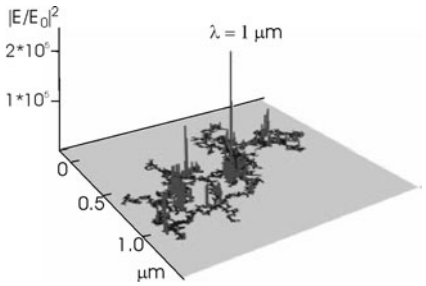

Figure 5. Typical SERS-active silver colloidal cluster and an estimate of the field distribution on such a silver cluster [57].

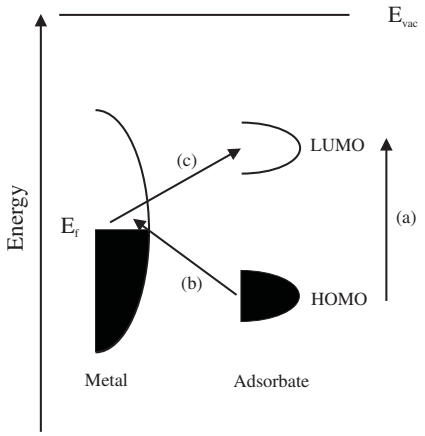

Figure 6. Energy level diagram for a 'molecule–metal system' showing also possible resonant Raman processes involving molecular states (path (a)) and molecular and metallic states (paths (b), (c)) [64].

to the best experimentally observed nonresonant SERS enhancement factors on the order of 10^{14} [18], which suggests the existence of additional enhancement mechanism(s) accounting for the missing factors.

Several different mechanisms are discussed as the origin of a 'chemical' or 'electronic' SERS effect, sometimes also called the first-layer effect since the mechanisms require direct contact between molecule and metal [5, 63, 64]. A possible enhancement mechanism is attributed to specific interactions, i.e. electronic coupling between molecule and metal and formation of an adsorbate–surface complex, resulting in an increased Raman cross section of the adsorbed molecule in the complex compared with the cross section of a 'free' molecule in a 'normal' Raman experiment. Other possible electronic SERS mechanisms involve a resonance Raman effect, which becomes operative due to shifted and broadened electronic levels in the adsorbed molecule compared with the free one or due to a new (charge transfer) electronic transition in the metal–molecule system [65,66]. Figure 6 shows a typical energy level diagram for a 'molecule–metal system', where the energies of the highest occupied molecular orbital (HOMO) and the lowest unoccupied molecular orbital (LUMO) are approximately symmetric relative to the Fermi level of the metal, together with possible resonant Raman processes involving molecular states (path (a)) and molecular and metallic states (paths (b), (c)) [64]. The figure also explains the change of the resonance conditions for paths (b) and (c) when the Fermi level is shifted, i.e. a potential-dependent SERS enhancement.

Another first-layer SERS effect is attributed to a so-called dynamical charge transfer [5, 63, 67], which can be described by the following four steps:

(a) photon annihilation, excitation of an electron into a hot-electron state,
(b) transfer of the hot electron into the LUMO of the molecule,
(c) transfer of the hot electron from the LUMO (with changed normal coordinates of some internal molecular vibrations) back to the metal and
(d) return of the electron to its initial state and Stokes photon creation.

Recent studies return to this mechanism in order to explain extremely large SERS enhancement factors in single-molecule SERS [21, 68]. In [68] atomic-scale roughness is discussed as a prerequisite for the chemical SERS enhancement based on dynamical charge transfer.

In general, the chemical SERS enhancement factor is considered to contribute enhancement factors on the order of 10–10^2 [64,69]. Recently, in the framework of dynamical charge transfer, it has been discussed that tunnelling electrons couple much more strongly to the molecular vibration than optical fields and that the cross sections for excitation of vibrations are about 10^{10}–10^{14} times stronger than the Raman cross section [68]. This would explain enhancement factors exploited in single-molecule SERS experiments. On the other hand, this dynamical charge transfer model does not explain the extremely strong enhancement factors of 10^{20} for hyper-RS, which can be easily understood in terms of an electromagnetic field enhancement model [61,62].

Frequency shifts, line widths and relative intensities of the Raman lines characterize the Raman spectrum of a molecule. As a consequence of possibly different enhancement mechanisms for different Raman modes, a SERS spectrum can show some deviations in relative intensities compared with a normal Raman spectrum of the same molecule. Due to the interaction between molecule and metal, Raman lines can be slightly shifted in frequency and changed in line width compared with a 'free' molecule. Strong field gradients can result in relaxed selection rules and in appearance of new normally forbidden Raman lines [70–72]. In many cases, SERS spectra show a higher depolarization ratio compared with spectra measured from a liquid [64,73].

In spite of all the small changes which can occur in a SERS spectrum, in most cases a SERS spectrum still provides a clear 'fingerprint' of the molecule, particularly also for biomedically relevant molecules.

2.2. SERS-active substrates for biophysical applications

The most common types of SERS-active substrate exhibiting the largest enhancement effects are clusters of colloidal silver and gold particles in the 10–100 nm size range, which are used in colloidal solution or 'dry' on a surface (see also figures 2(b) and 4). Colloidal silver and gold particles are made by different chemical reduction processes [74,75] or by laser ablation from solid silver or gold [76,77], where ablation has the advantage of generating 'chemically clean' colloidal surfaces. Chemical colloid preparation results in 'impurity molecules' on the surface of the colloidal particles such as for instance citrate, which has been introduced during the reduction process. In single-molecule experiments, SERS signals of these impurity molecules appear at about the same level as the Raman spectra of the target molecule [13,78]. In addition to the nanoscale roughness of the metal, which is a prerequisite for the electromagnetic field enhancement, 'atomic-scale roughness', so-called SERS-active sites, seems to play an important role in first-layer SERS mechanisms [68]. In some experiments, the addition of salts considerably increases the enhancement effect since ions may provide active sites [9]. There are experimental observations that small silver ion clusters and their complexes with ions such as I^- give rise to a strong chemical SERS enhancement [79–81].

Other very common SERS-active substrates providing nanoscale and atomic-scale roughness include evaporated island films of silver and gold or electrodes of these metals. Gold and silver electrodes do not provide such extremely large enhancement factors ($>10^{12}$) as silver or gold colloidal clusters or island films but they have the advantage of adjusting their surface potential in order to study charge transfer processes between the target molecule and the metal surface.

Silver modification of thin-layer chromatography (TLC) materials can make these plates SERS active and allow a combination of TLC and SERS [82,83]. SERS-active substrates can also be made from photographic silver halide materials. SERS-active silver nanoparticles and atomic-scale silver clusters are generated *in situ* by the excitation laser [84–86].

Also interesting are so-called 'SERS optical fibre probes', where the end of an optical fibre is covered by a SERS-active substrate, resulting in enhanced Raman signals collected by the fibre [87, 88].

SERS microprobes have been designed in micrometre dimensions as metal films on silicon substrates for insertion into small openings or as silver wire microelectrodes as small as 0.75 μm [89, 90]. For example, such SERS probes are small enough and provide useful geometry and mechanical strength and flexibility for direct insertion in lipid secreting structures and to probe lipid chemistry [90].

Recently, SERS effects have been reported from sputtered silver oxide layers after photoactivation [91, 92].

Surface-enhanced Raman signal can be also measured using a fine metal tip, such as AFM or STM tips, approaching a layer of the target molecules within a few nanometres [93–98]

Most interesting SERS-active structures exhibiting well defined and controlled plasmon resonances might be nanoparticle arrays fabricated by nanosphere lithography (NSL) [99]. For example, the gap mode in closely spaced particles can provide enhanced optical fields in nanometric spots [100].

For application of SERS in biophysics SERS-active substrates need to be developed, which are not only compatible with the geometry and size of the sample; SERS-active substrates need to also be 'chemically' compatible to a 'biological environment'. In general, due to its chemical inactivity, gold should be the more suitable metal for incorporation inside biophysical systems. It was shown that gold colloidal clusters have comparably good SERS enhancement factors as silver clusters when NIR excitation is applied [101]. Moreover, NIR would be the desired excitation range for Raman measurements in biological environment since the lower-energy photons reduce the fluorescence background in biological samples and also the risk of degeneration.

2.3. Anti-Stokes SERS—a two-photon Raman probe for biophysics

Two-photon spectroscopy can provide several advantages, particularly also in biophysical/biomedical spectroscopy. During the last decade, two-photon excited fluorescence became a widely used technique [102]. Recently, coherent anti-Stokes Raman scattering (CARS) has been demonstrated to be a very promising nonlinear Raman spectroscopic tool for biophysics studies [103–106].

Exploiting extremely high effective SERS cross sections, surface-enhanced anti-Stokes RS can become an incoherent two-photon Raman probe: as we briefly discussed in figure 1, Stokes and anti-Stokes RS start from the vibrational ground and first excited vibrational level, respectively. In addition to the thermal Boltzmann population, first excited vibrational levels can be measurably populated by a very strong surface-enhanced Raman process.

Figure 7 schematically shows Stokes and anti-Stokes RS and the rate equation describing the population and depopulation of the first excited vibrational level by Raman Stokes and anti-Stokes transitions. Assuming steady state and weak saturation (cw laser experiment), the anti-Stokes SERS signal P_{aS}^{SERS} and the Stokes SERS signal P_{S}^{SERS} signal can be written as [14]

$$P_{aS}^{\mathrm{SERS}} = (N_0 \mathrm{e}^{-\frac{h\nu_M}{kT}} + N_0 \sigma_S^{\mathrm{SERS}} \tau_1 n_L) \sigma_{aS}^{\mathrm{SERS}} n_L \tag{5a}$$

$$P_{S}^{\mathrm{SERS}} = N_0 \sigma_S^{\mathrm{SERS}} n_L \tag{5b}$$

where τ_1 the lifetime of the first excited vibrational state, n_L is the number of laser photons cm^{-2} s^{-1}, T is the sample temperature (300 K) and h and k are the Planck and Boltzmann constant, respectively. The second term on the right-hand side of equation (5*a*) describes 'SERS population' of the first excited vibrational state in excess to the Boltzmann population. In 'normal' RS this term can be neglected compared with the thermal population

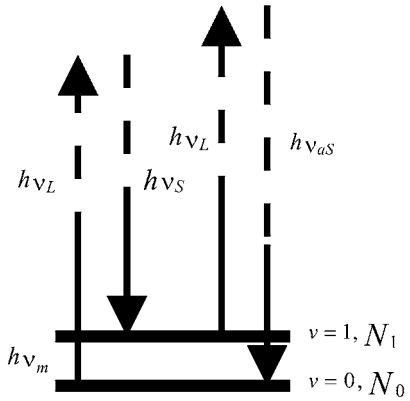

$$\frac{dN_1}{dt} = (N_0 - N_1)\,\sigma^{SERS} n_L - \frac{N_1}{\tau_1}$$

Figure 7. Schematic Stokes- and anti-Stokes RS and the rate equation describing the population and depopulation of the first excited vibrational level by Raman Stokes and anti-Stokes transitions.

(first term), since for 'normal' RS $\sigma^{\mathrm{RS}}(\nu_m)\tau_1(\nu_m)$ is on the order of 10^{-40} cm^2 s^{-1}. This means that about 10^{38} laser photons cm^{-2} s^{-1} (about 10^{20} W cm^{-2} excitation intensity) are required to make the Raman pumping comparable to the thermal population of the first vibrational level. However, effective SERS cross sections on the order of 10^{-16} cm^2 bring the product from cross section and vibrational lifetime $\sigma^{\mathrm{SERS}}(\nu_m)\tau_1(\nu_m)$ to 10^{-27} cm^2 s and make the 'pumping term' comparable to the Boltzmann term or even dominant. This anti-Stokes RS starting from 'pumped' vibrational levels is a two-photon Raman process: one photon populates the excited vibrational state; a second photon generates the anti-Stokes scattering. The anti-Stokes signal P_{aS} depends quadratically on the excitation laser intensity whereas the Stokes signal P_S remains linearly dependent. Figure 8 shows plots of anti-Stokes and Stokes signal powers of crystal violet on colloidal gold clusters versus excitation laser intensities.

We can write equation (5*a*), using an effective two-photon cross section $\sigma^{\mathrm{SERS}}_{aS,nl}$,

$$P^{\mathrm{SERS}}_{aS,nl} = N_0 \sigma^{\mathrm{SERS}}_{aS,nl} n_L^2 \tag{6}$$

with

$$\sigma^{\mathrm{SERS}}_{aS,nl} = \sigma^{\mathrm{SERS}}_{S} \sigma^{\mathrm{SERS}}_{aS} \tau_1. \tag{6a}$$

Assuming a SERS cross section of approximately 10^{-16} cm^2 and a vibrational lifetime on the order of 10 ps, effective twophoton cross sections can be inferred to be about 10^{-43} cm^4 s. This provides a two-photon excited Raman probe at a cross section more than seven orders of magnitude larger than typical cross sections for two-photon excited fluorescence [107]. The large effective cross section can be explained by the nature of the process, which is a two-photon process exploiting the vibrational level as a real intermediate state.

Because of its very high cross section, this two-photon Raman effect can be observed at relatively low excitation intensities using cw lasers.

Surface-enhanced pumped anti-Stokes Raman spectroscopy provides all the peculiarities of a two-photon probe, such as an inherently confined probed volume compared with one-photon surface-enhanced Stokes scattering as well as a linear increase of the spectroscopic

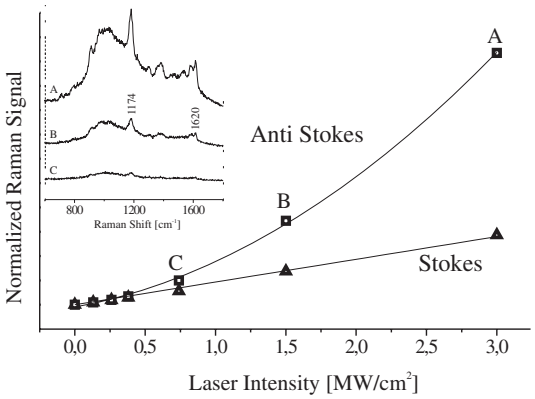

Figure 8. Anti-Stokes and Stokes signal powers of crystal violet on colloidal gold clusters versus excitation laser intensities. The lines indicate quadratic and linear fits to the experimental data, displaying the predicted quadratic and linear dependence. The inset shows the unprocessed spectra at different excitation laser intensities demonstrating the increase of the spectroscopic signal relative to the background for increasing excitation intensities.

signal relative to the background for increasing excitation intensities. In general, the advantages of two-photon Raman spectroscopy, particularly in the biomedical field, are the same as discussed for two-photon excited fluorescence spectroscopy [102, 107]. Moreover, anti-Stokes spectra are measured at the high-energy side of the excitation laser, which is free from fluorescence, since two-photon excited fluorescence appears at much higher frequencies.

2.4. SERS—a single-molecule tool

In general, SERS-enhancement factors on the order of 10^{14} corresponding to effective SERS cross sections of about 10^{-16} cm^2/molecule allow Raman detection of single molecules. Figure 9 shows a schematic diagram of an experimental set-up used for single-molecule NIR SERS spectroscopy. SERS-active substrates are silver or gold colloidal cluster structures in different sizes as shown in figures 2(b), 4 and 5. The clusters can be used in water or 'dry' on a surface. Clusters exceeding a particular size (about 150 nm) provide uniform enhancement factors independent of cluster size [18]. The uniform enhancement explains the relatively well quantized SERS signals for one-, two- and three-molecule scattering events in single-molecule Raman experiments [15, 17].

In our first example, shown in figure 10(a), single adenine molecules are attached to silver colloidal clusters as shown in the magnification glass in figure 9. Adenine is added to the aqueous solution of such cluster at very low concentration resulting in clusters carrying zero or only one adenine molecules and in average of about one molecule in the probed volume. Brownian motion of these clusters into and out of the probed volume results in strong statistical changes in SERS signals measured from such a sample in time sequence. Figure 10(a) shows selected typical spectra collected in 1 s representing 0, 1, 2 molecule scattering and the statistical analysis of 100 measurements of the SERS signal at the 735 cm^{-1} adenine ring breathing mode. The Poisson distribution of the Raman signal reflects the probability of finding zero, one, two (or three) molecules in the scattering volume during the actual measurement and is evidence that single-molecule detection of adenine by SERS is achieved. As expected, the Raman signal from a sample at ten times higher adenine concentration (18 molecules in the probed volume) could be fitted by one Gaussian curve (dotted curve in figure 10(a)) since the number

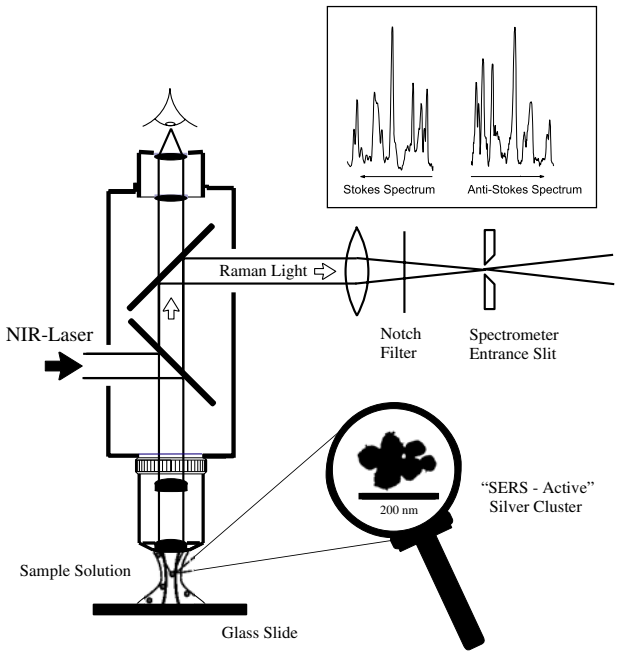

Figure 9. Schematic diagram of a single-molecule SERS experiment; a microscope is used for laser excitation and collection of the Raman scattered light.

of molecules in the probed volume remains statistically constant.

It is also interesting to compare the maximum number of photons emitted by a molecule in fluorescence or Raman process under saturation conditions, which is inversely proportional to the lifetime of the excited states involved in the optical process. Due to the shorter vibrational relaxation times compared with electronic relaxation times, a molecule can perform more Raman than fluorescence cycles per time interval [13, 78]. Therefore, the number of Raman photons per unit time which can be emitted by a molecule under saturation conditions can be higher than the number of fluorescence photons by factors 10^2–10^3. This allows shorter integration times for detecting a molecule or higher rates for counting single molecules. Of course, due to shorter vibrational lifetimes, the saturation intensity for a SERS process will be higher than for fluorescence, but higher excitation intensities up to saturation should not be a problem in SERS because the applied NIR photons are not in resonance with molecular transitions, which avoids photodecomposition of the probed molecule.

Another approach in single-molecule RS exploits surface-enhanced RRS [16,21]. SERRS spectra of single Rhodamine 6G molecules were measured from small 'hot silver particles', where the hot particles are very probably created by aggregation of a few, at least two, colloidal particles. Figure 10(b) shows a SERRS spectrum of a single haemoglobin molecule [108].

3. Examples for application of SERS in biophysics, biochemistry and biomedicine

SERS applications in the biophysical/biochemical and biomedical field up to the middle of the 1990s are summarized in several review papers [36–40, 109, 110]. The reviews discuss SERS experiments performed on amino acids and peptides, on purine and pyrimidine bases, but also on 'large' molecules such as proteins, DNA and RNA. SERS was also studied from many 'intrinsically coloured' biomolecules such as chlorophylls and other pigments, as well

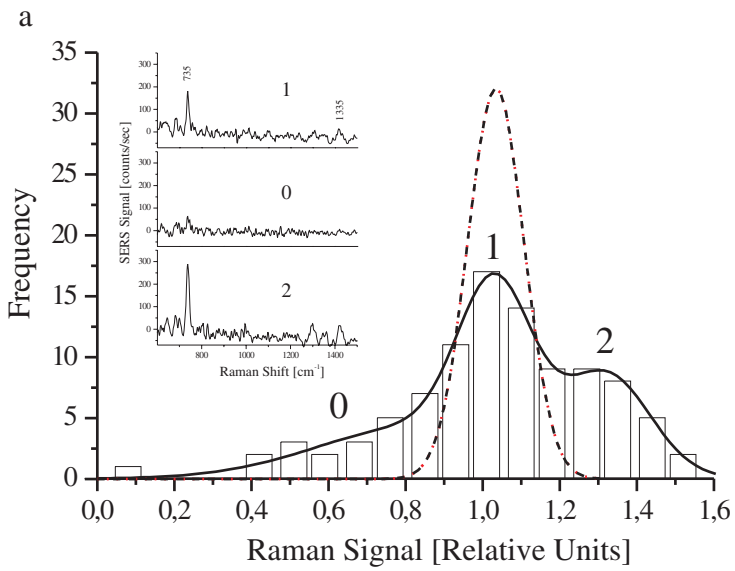

Figure 10. (a) SERS spectra of single adenine molecules on colloidal silver clusters. The inset shows typical '1', '0' and '2' molecule spectra measured in 1 s collection time at 830 nm excitation using a power of about 100 mW. Statistical analysis of 100 SERS measurements at an average of 1.8 adenine molecules in the probed volume. The x-axis is divided into bins whose widths are 5% of the maximum signal. The y-axis displays the frequency of the appearance of the appropriate signal levels of the bins. The experimental data of the 1.8-molecule sample were fitted by the sum of three Gaussian curves (solid curve), whose gradation of the areas is roughly consistent with a Poisson distribution for an average number of 1.3 molecules. The dotted curve shows the experimental statistical Gaussian distribution of the SERS signal from 18 adenine molecules in the probed volume. (b) SERS spectrum of a single haemoglobin molecule on a silver nanoparticle dimer (see inset) measured in 200 s at 514.5 nm excitation laser wavelength using $\sim$20 μW laser power [108].

(This figure is in colour only in the electronic version)

as from larger molecules containing chromophores such as the haem-containing proteins.

Other, more medical, applications include SERS detection of stimulating drugs [111] and selective analysis of antitumour drug interaction with DNA [112–116].

SERS is not only of interest as a method for ultrasensitive detection and structural characterization of 'biomolecules'; the technique has been also applied to study biophysically interesting processes. For example, SERS can be used to monitor transport through membranes. The results show that SERS can discriminate between the movement of different molecules across a membrane and to observe different interfacial arrival times and concentration growth rates in the receiving (colloidal silver) solution [117].

SERS represents also an interesting approach for studying charge transfer processes, for instance in cytochrome c, which has been extensively investigated on bare and coated silver electrodes [33]. In particular, the selectivity of SERRS allows the determination of the interfacial potential-dependent equilibria and reactions by probing the vibrational spectra of the haem group of the adsorbed cyt-c exclusively. Recently, time-resolved SERRS was used to study the kinetics of the heterogeneous electron transfer between cyt-c and a SAM-coated silver electrode, in particular the electric field dependence of the interfacial charge transfer [35].

In the following, we discuss selected examples of biophysical/biomedical applications of SERS which have been performed during the last half decade.

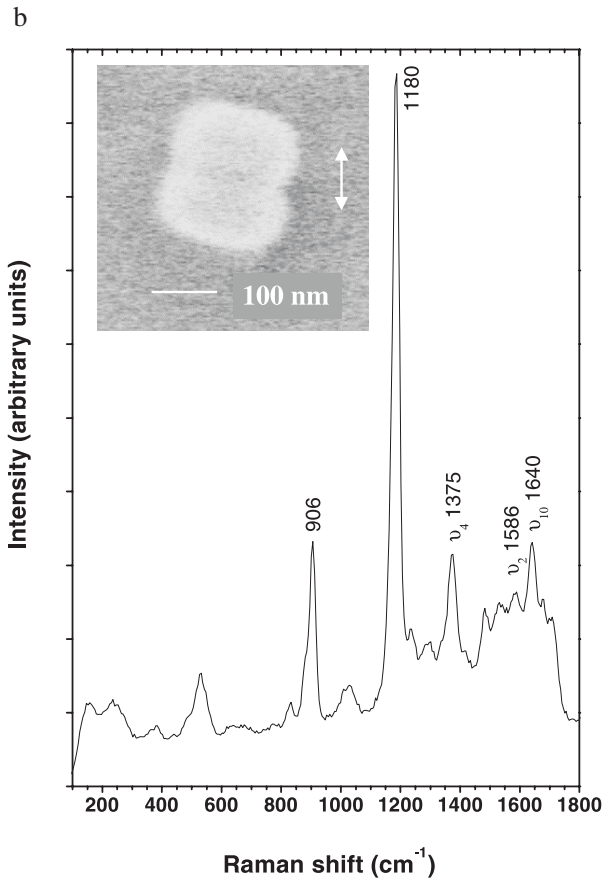

Figure 10. (Continued.)

3.1. Detection and identification of neurotransmitters

The detection, identification and quantification of neurotransmitters in brain fluid is an important question in neurochemistry. Of particular interest are measurements of concentration changes in correlation to neuronal events, i.e. measurements on the timescale of neuronal processes [118]. For example, the extracellular concentration of the neurotransmitter glutamate is most sensitive and indicative of injuries involving the central nervous system. It has been shown that artificial neural networks are capable of accurately identifying the Raman spectra of aqueous solutions of different neurotransmitters [119]. However, the detection limits in spontaneous RS are on the order of 10^{-1} M concentrations, i.e. orders of magnitude higher than physiologically relevant values. The detection limits could be decreased by many orders of magnitude by exploiting the SERS effect. SERS spectra of different neurotransmitters have been measured on silver electrodes and on colloidal silver particles in water [120–124].

Figure 11 shows SERS spectra of dopamine and norepinephrine in aqueous solution of colloidal silver clusters. SERS spectra of these two neurotransmitters were measured at concentrations between 5×10^{-6} and 5×10^{-9} M with accumulation times as short as 0.025 s [123]. Probed volumes were in a size of about 200 pl, which results in fewer than 10^6 molecules (atomols) contributing to the Raman signal. Recently, similar detection

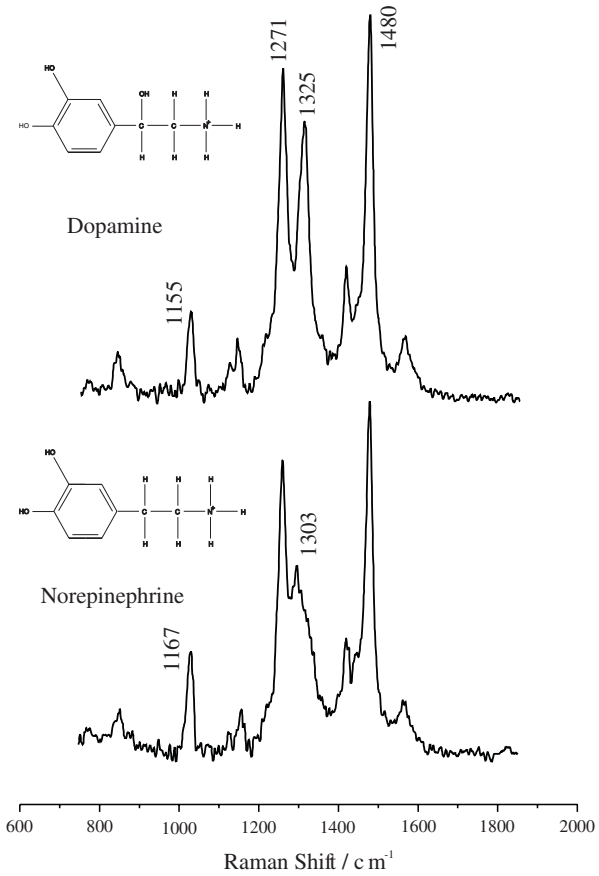

Figure 11. SERS spectra of neurotransmitters in silver colloidal solution. Spectra were collected in 50 ms using 100 mW NIR excitation.

limits for dopamine and epinephrine have been reported from two-photon-excited fluorescence experiments [125]. In the SERS experiments, albumin was added as a protein component to the aqueous sample solutions in order to make them more similar to a real biological environment. The low concentrations and fast data acquisition are on the order of physiologically relevant concentrations and close to the timescale of neuronal events, respectively.

In spite of their very similar chemical structure and very similar 'normal' Raman spectra of dopamine and norepinephrine, clear differences appear between the SERS spectra of these catecholamine transmitters. Such differences are probably due to small differences in the adsorption behaviour of these molecules. SERS, therefore, can improve the structural sensitivity and selectivity for similarly structured molecules. SERS spectra from mixtures containing the two neurotransmitters allowed quantitative information on the mixtures of the two compounds.

Using SERS in colloidal silver solutions, glutamate has been detected in microdialysis samples of rat brains in 0.4–5 μM concentration [124]. Normal physiological concentration levels in rats are expected to be in the same range.

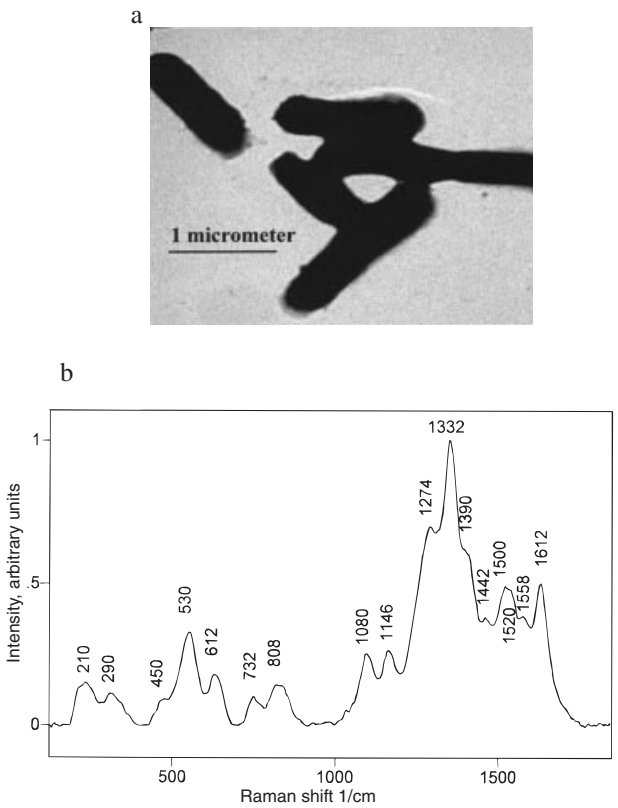

Figure 12. Electron microscopic view (a) and SERS spectrum (b) of *Escherichia coli* coated with a silver colloid [128].

3.2. SERS detection and identification of microorganisms

Fast identification and characterization of bacteria is a matter of serious interest. Particularly, the increasing frequency of infections in hospitals stimulates the search for new powerful and rapid methods for identification of bacteria as a first step for a directed antibiotic attack. Techniques for characterizing bacteria are based on morphology, biochemical tests and vibrational spectroscopy. Fourier transform infra-red (FTIR) absorption spectroscopy [126] and UV resonance Raman spectroscopy [127] have been used for vibrational spectroscopic characterization of micro-organisms, but SERS spectroscopy should also be a valuable tool for identifying bacteria based on their vibrational spectrum. In particular, the high sensitivity of SERS provides hope of needing only relatively small amounts of bacteria for the identification procedure. First SERS studies of bacteria were reported in 1998 [128]. In this study, silver colloidal particles are produced selectively within the bacterium or on its wall, forming there a rough silver coating. Figure 12 shows the SERS spectrum and the TEM of *Escherichia coli* with a wall colloid. The Raman signal of the bacterial wall must have been enhanced by many orders of magnitude. SERS spectra as in figure 12 are typically collected in a few seconds using 1–2 mW 514.5 nm argon laser excitation. For comparison, Raman measurements on untreated cells result in much weaker spectra using even 100 mW laser power and 30–60 min collection time. Considering the number and diversity of biomolecules in the bacterial wall, the SERS spectrum in figure 12 also demonstrates that SERS is a selective effect, showing predominantly those molecules and functional groups that are in the immediate proximity of

the silver colloid. For example, the strong line at 1332 cm^{-1} is assigned to proteins and protein components [128]. For comparison, UV resonance Raman is also selective, but the resonance Raman effect favours vibrational modes associated with the chromophore.

SERS spectra of *E. coli* K12 in contact with citrate and borohydride-reduced silver colloids as well as in contact with colloidal gold are reported in [129]. In this study, 632.8 nm excitation was applied at low laser powers, allowing measurements on living bacteria. Very good signal to noise SERS spectra have been recorded in a few minutes. The SERS spectra are comparably good for silver and gold. The study also compares a beta-lactam-resistant *E. coli* TEM-1 strain and a beta-lactam-susceptible *E. coli* strain. Both strains show slight differences in their SERS spectra in the low-frequency region and changes in the relative line strengths, demonstrating the high structural selectivity of SERS.

3.3. Immunoassays utilizing SERS

In many cases, immunoassays require the concomitant detection of several label molecules (reporters) in order to detect multiple antigens. Because of its high structural selectivity and its high sensitivity, SERS has the potential to serve as a nearly perfect read-out method for the labels. The first application of SERS in an immunoassay of human thyroid-stimulating hormone (TSH) was reported already in 1989 [130]. In this early experiment, the 'SERS-active substrate' was a silver film, which had been coated with anti-TSH antibodies and then incubated with TSH. A second anti-TSH labelled with *p*-dimethylaminoazobenzene was added to bind to the TSH. The SERRS signal of the label was used to quantify TSH.

Figure 13(a) describes another type of assay, where colloidal gold, maybe supported by the gold surface, serves as the 'SERS-active substrate'. Immobilized antibodies on the gold surface capture antigens from solution. Gold nanoparticles labelled with both specific antibodies and a specific reporter bind to the captured antigen. By immobilizing different antibodies and using different reporters, the presence of different antigens can be detected by the characteristic surface-enhanced Raman spectrum of the specific reporter molecules. There are several potential advantages of using SERS as a read-out method compared with other techniques, such as fluorescence labels. A SERS spectrum shows very specific and narrow Raman lines, minimizing the spectroscopic overlap of different labels. Moreover, excitation of a SERS process allows the use of a single excitation source for multiple labels. As a further advantage, as a Raman process, SERS is not sensitive to any quenching process or photobleaching. Figure 13(b) shows SERS spectra of three types of reporter-labelled immunogold colloids in comparison with the 'empty' spectrum of commercial gold colloids conjugated with goat anti-rat IgG [131]. The spectra show clearly distinguishable spectral features for the three different labels.

Reference [132] describes an enzyme immunoassay employing SERS spectra of the enzyme reaction product. Antibodies immobilized on a solid substrate bind antigen (mouse-IgG) which binds to a second antibody labelled with peroxidase. If these immunocomplexes are subjected to reaction with *o*-phenylenediamine, azoaniline is generated. The reaction product is adsorbed on colloidal silver particles, resulting in a strong SERS spectrum of azoaniline, of which the signal strength is proportional to the concentration of the antigen.

The method of silver colloidal SERS of the enzymatic product has been applied to the direct detection of enzymes in cells [133]. The method was successfully used to detect and to quantify prostaglandin H synthase-1 and 2 (PGSH-1 and 2) in normal human hepatocytes and human hepatocellular carcinoma (HepG2) cells.

3.4. DNA and gene probes based on SERS labels

Progress in DNA and genome research results in a strong need for methods for the detection and quantification of DNA and for the development of techniques for rapid characterization of

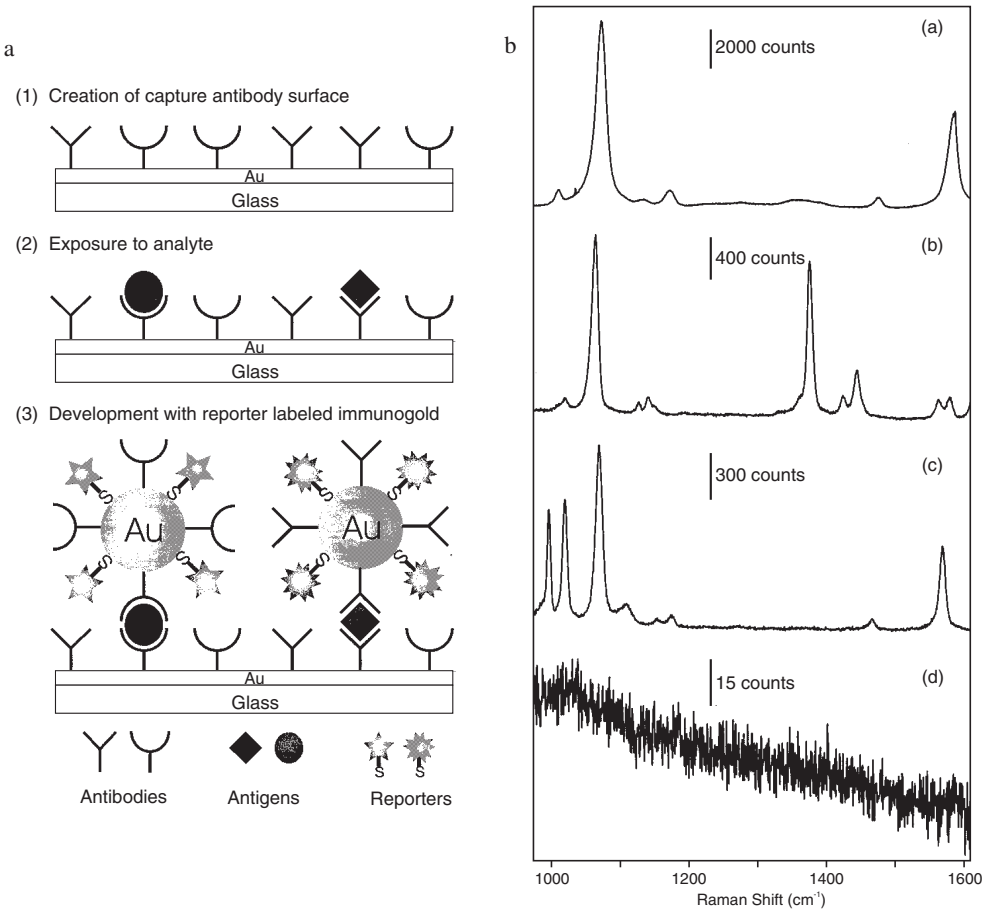

Figure 13. (a) Scheme of an immunoassay system using two different SERS labels. (b) SERS signatures of three types of reporter-labelled immunogold colloid: (a) MBA/goat anti-rat IgG, (b) NT/goat anti-rat IgG, (c) TP/goat anti-rabbit IgG, (d) goat anti-rat IgG [131].

DNA fragments. For example, quantification of the DNA is of interest during polymerase chain reactions (PCRs). [134] proposes a SERS-based method for monitoring the concentration of double-stranded (ds-) DNA amplified by PCR. In the proposed method, a DNA intercalator, $4', 6$-diamidino 2-phenylindole dihydrochloride (DAPI), was employed in order to form a complex with the ds-DNA. DAPI gives rise to a strong SERS signal in silver colloid solution but it is also a so-called deeply intercalating dye. Such strong intercalation prevents a strong contact between DAPI and silver colloids, and the SERS signal of the dye vanishes with intercalation. Therefore, the SERS signal of the intercalator is inversely proportional to the concentration of ds-DNA. A good straight line fit was obtained between DAPI SERS signals versus concentration of ds-DNA amplified by PCR.

Methods for characterizing DNA fragments and for detecting specific nucleic acid sequences in fast screening procedures are mainly based on hybridization of the target DNA fragments to complementary probe sequences, which are tagged with specific labels. Labelling can include radioactive or fluorescence reporters [135]. Recently, quantum dots and nanoparticles have been suggested as interesting new fluorescence labels [136, 137]. As discussed in

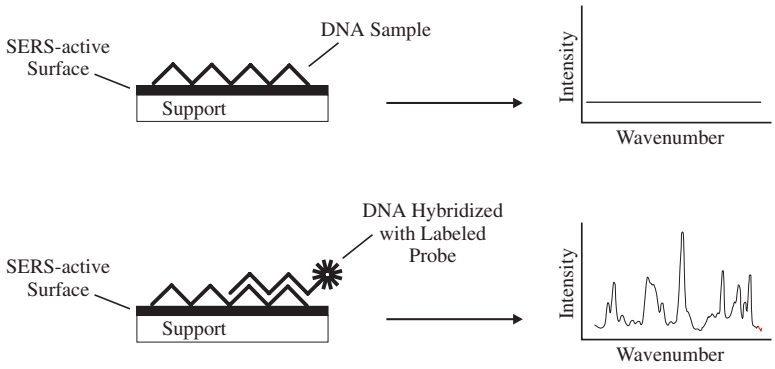

Figure 14. Schematic diagram of DNA hybridization detection using a SERS label [138].

section 3.4, replacing fluorescence labels by SERS labels may offer several advantages, particularly for a multiplex screening and simultaneous detection of different sequences. Figure 14 shows a schematic diagram of a DNA probe exploiting a SERS label [138].

In [139], SERS has been applied in hybridization experiments for detecting $p(dA)_{18}$. The oligonucleotides have been attached on a nitrocellulose surface. Nucleic acid fragments consisting of 18 deoxyribonucleotide oligomers of thymine, $p(dT)_{18}$, which is the appropriate mirror strand, have been tagged with cresyl fast violet (CFV) as the SERS label. The labelled $p(dT)_{18}$ that did not hybridize to the $p(dA)_{18}$ oligomers were removed by washing the nitrocellulose. The hybridized oligomers were deposited on a SERS-active silver substrate. A strong SERS peak appears from the labelled $p(dT)_{18}$. For example, labelled $p(dC)_9$ oligonucleotides were also used and no SERS signal was detected since $p(dC)_9$ oligonucleotides do not hybridize to $p(dA)_{18}$.

The effectiveness of the SERS gene technique was demonstrated in experiments using the human immunodeficiency virus (HIV) gag gene sequence. The authors discuss the results of this study as potentially useful for HIV detection by SERS gene probes [140].

Exploiting $2, 5, 1', 3', 7', 9'$-hexachloro-6-carboxyfluorescein (HEX) and Rhodamine 6G as label molecules, it was possible to detect a 2×10^{-12} M solution of labelled DNA using SERRS [141].

3.5. Probing DNA and DNA fragments without labelling based on their intrinsic Raman spectra

First SERS spectra of DNA adsorbed on a silver electrode were reported in 1981 [142]. During the 1980s several papers discussed SERS studies of nucleic acids and their components [37, 143–145]. Silver electrodes and colloidal silver particles in aqueous solution served as the most common SERS-active substrates. In many experiments, the silver surface is not only responsible for the SERS enhancement. It can also give rise to structural changes of the adsorbed nucleic acids, such as denaturation [142, 144]. In experiments performed on colloidal silver, it can sometimes take hours and even days between addition of the target molecule to the silver colloidal solution and the appearance of a stationary SERS spectrum [145]. This effect, which has been found particularly for RNA, has been explained by the time needed for the various molecules to adsorb on a side providing large enough enhancement level.

In a more recent study, SERS on electrochemically roughened silver surfaces was applied to detect a single mismatch in a ds-DNA fragment (209 base pairs) without the use of any label molecule [146]. SERS spectra originated from the 'open region' around the mismatch (A–G) in the DNA fragment show strong adenine and cytosine Raman lines in contrast to

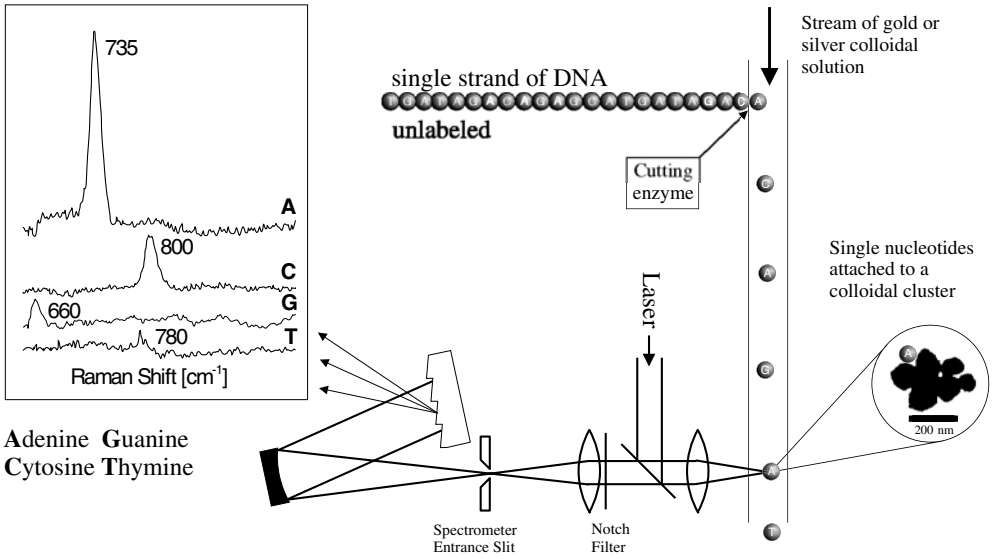

Figure 15. Idea of a rapid sequencer based upon surface-enhanced RS from single DNA bases. Single nucleotides are cleaved and attached to colloidal silver or gold clusters, which flow through the laser focus and are detected in order of cleaving.

SERS spectra of a perfectly matched DNA fragment. The observation is in agreement with SERS spectra measured for native and denatured DNA, where the appearance of the strong adenine ring breathing line indicates denaturation [142, 143].

In most of the SERS studies the target nucleic acids were applied in relatively high concentrations (10^{-5}–10^{-8} mol l^{-1}), but the most interesting aspects of SERS on nucleic acids might be attributed to the ultrasensitive and single-molecule capabilities of the method.

In section 2.4 single-molecule detection of adenine and adenosine monophosphate (AMP) was demonstrated [18]. To detect and to identify single bases by fluorescence, they must be labelled by fluorescent dye molecules to achieve large enough fluorescence quantum yields and distinguishable spectral properties [147].

The strong field enhancement provided by colloidal clusters might be the key effect for the enormous non-resonant surface-enhanced Raman cross sections exploited in single-molecule adenine experiments. Therefore, it should be possible to achieve SERS cross sections on the same order of magnitude for other bases when they are attached to colloidal silver or gold clusters. The nucleotide bases show well distinguished surface-enhanced Raman spectra [148, 149], also shown in figure 15. Thus, after cleaving single native nucleotides from a DNA or RNA strand into a medium containing colloidal silver clusters (for instance, into a flowing stream of colloidal solution or onto a moving surface with silver or gold cluster structure), detection and identification of single native nucleotides should be possible due to unique SERS spectra of their bases. Figure 15 illustrates the idea of a rapid sequencer base upon surface-enhanced RS from single DNA bases.

3.6. SERS studies inside living human cells

SERS studies have also been performed on living cells [112, 114]. In these experiments, colloidal silver particles were incorporated inside the cells and SERS was applied to monitor the intracellular distribution of drugs in the whole cell and to study the antitumour drugs/nucleic

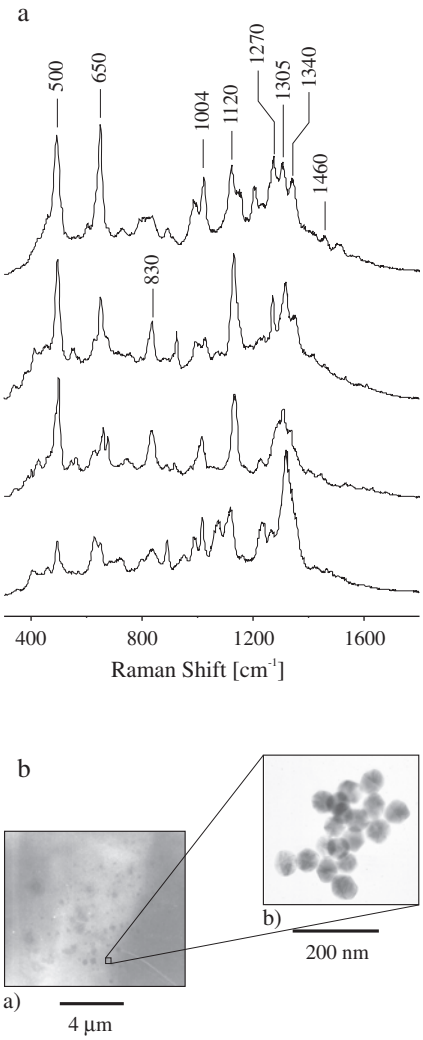

Figure 16. (a) SERS spectra measured with 1 μm spot size from different places on a cell monolayer incubated with colloidal gold; (b) electron micrographs of colloidal gold particles inside a cell monolayer. The higher magnification shows that the gold particles are aggregates of 60 nm colloidal spheres [151].

acid complexes. Surprisingly, these experiments show SERS spectra of the drug/DNA complexes represented by Raman lines of the drugs but no SERS spectra of the native cell constituents themselves were detected. Weak SERS bands attributed to phenylalanine and amide I and III bands were measured in the strong SERS spectra of dimethylcrocetin (DMCRT) in a living HL 60 cell in contact with a gold island film [150].

Figure 16(a) shows Raman spectra measured from different places on a cell monolayer (intestinal epithelial cells HT29) incubated with colloidal gold [151]. The strongly enhanced Raman signals allow Raman measurements in the 400–1800 cm^{-1} range with 1 μm lateral resolution in 1 s or shorter collection times using 3–5 mW NIR excitation. SERS mapping over a cell monolayer with 1 μm lateral resolution shows different Raman spectra at almost all places, reflecting the very inhomogeneous chemical constitution of the cells. The Raman

lines can be assigned to native chemical constituents in the cell nucleus and cytoplasm, such as DNA, RNA, phenylalanine, tyrosine etc. For the experiments, 60 nm gold nanoparticles were incorporated in the cells by fluid-phase uptake during the growing process, where the culture medium was supplemented with the colloidal gold suspension. The salts in the buffer solution induce the formation of small colloidal aggregates with sizes of a few hundred nanometres. Cluster–cluster aggregation inside the cell results in the formation of larger gold colloidal clusters as shown in figure 15(b). Evidence that cells are alive after treatment with the colloidal gold comes from phase contrast inspection of the cultures showing that cells incubated with colloidal gold are visibly growing and that there is no evidence of cell rounding, apoptotic activity or cell detachment from the growth surface when compared with control monolayers.

The reported experiments demonstrate the feasibility of measuring SERS of native constituents within a single viable cell using colloidal gold particles as SERS-active nanostructures and generating a surface-enhanced Raman image inside a living cell. In general, ultrasensitive Raman spectroscopy inside living cells should allow for monitoring small chemical changes in the cell which could be the precursors of larger morphological changes, visible by conventional microscopy. In this way, exciting opportunities might be opened up for the diagnosis of diseases such as cancer to be made at earlier stages than previously possible.

4. Summary, prospects and limitations of SERS in biophysics

Surface-enhanced RS was discovered about 25 years ago and is now a well established phenomenon. In general, as a laser spectroscopic technique, SERS can be applied under 'biophysically ambient conditions' (atmosphere, aqueous liquids, room temperature) and in a 'biological environment'. SERS spectra measured in a time-resolved regime allow us to monitor time-dependent biophysical processes and detect short-lived intermediate species.

In general, using a confocal microscope, Raman and SERS signals can be observed from volumes of approximately the cube of the wavelength, enabling spatially resolved measurements in cells, chromosomes and microorganisms [128, 129, 151]. Compared with 'normal' Raman spectroscopy of cells [152, 153], the strongly enhanced signal in SERS allows orders of magnitude shorter collection times (1 s or less per mapping point) providing the opportunity of Raman mapping over a cell in a realistic timescale for monitoring small chemical changes in the cell. Of course, the SERS requires the presence of 'SERS-active' nanostructures, where in the biomedical field gold nanoparticles might be a favourite choice.

In spite of the fact that some of the experimental observations in SERS still create some controversy and are not yet completely understood, the effect attracts rapidly growing interest as a spectroscopic method, particularly also in biophysics and life sciences.

Most exciting for biophysical studies might be the trace analytical capabilities of SERS, which allow us to establish the molecular identity at the single-molecule level. This is of great interest since biologically relevant molecules are often available for characterization in extremely small amounts only. For example, a spectroscopic method for characterizing very small amounts of DNA would open exciting opportunities for reducing or even avoiding the PCR amplification.

SERS provides a complementary technique to fluorescence, which is widely used as an ultrasensitive and single-molecule spectroscopic tool in biophysics. To detect and to identify single molecules by fluorescence, in many cases they must be labelled by fluorescent dye molecules to achieve large enough fluorescence quantum yields and distinguishable spectral properties. SERS is a method for detecting and identifying a molecule which does not require

any labelling because it is based on the intrinsic SERS of the molecule.

Due to the mainly electromagnetic origin of the enhancement, it should be possible to achieve a strong SERS effect for each molecule. However, there is still a molecular selectivity of the effect, which cannot be explained yet. Based on empirical findings, SERS seems to work very well for molecules with delocalized pi electrons. Therefore, fortunately, SERS should be applicable for relatively many problems in the biomedical field.

But also, if labelling of the target 'biomolecule' should be applied for any reason, 'SERS labels' can provide several advantages compared with fluorescence tags. Because of the high specificity of a Raman spectrum, spectral overlap between different labels is very unlikely, even when their molecular structures are very similar. This results in a huge arsenal of potential SERS labels, allowing a real multiplex detection in screening processes. As a further advantage, SERS is a nonresonant process and the effect is therefore insensitive to photobleaching and self-quenching of the marker molecule, which can become serious problems in fluorescence spectroscopy.

Limitations of SERS spectroscopy are attributed to the fact that target molecules have to be attached to so-called 'SERS-active substrates' such as nanometer-sized silver or gold structures. On the other hand, performing spectroscopy in the local optical fields of the nanostructures provides the most exciting capabilities of the effect in biophysics. In SERS, lateral resolution is determined not by the diffraction limit, but by the spatial confinement of the local fields. For special nanostructures this field confinement can be smaller than 10 nm, suggesting the opportunity for selective Raman probing of parts of large biomolecules.

In principle, the high local optical fields open up interesting opportunities for each kind of spectroscopy. For example, the field enhancement effect is also operative in fluorescence. The effect of surface-enhanced fluorescence has been observed for a few molecules [154–156]. However, in many cases, the metal provides strong nonradiative decay channels. This fluorescence quenching effect can overcompensate the field enhancement, and the net fluorescence signal observed for molecules attached to a metallic nanostructure is much smaller than that measured without the metal. Since quenching effects and field enhancement have a different dependence on the distance to the metal (the quenching effect decreases faster with increasing distance), the fluorescence signal can be controlled and optimized by defined spacers between metal and fluorophore.

High local optical fields provide particularly attractive opportunities for nonlinear or two-photon spectroscopy, where the signal depends on the enhanced field intensities raised to a power of two or greater. For example, surface-enhanced two-photon fluorescence [98] and surface-enhanced hyper-RS [62] might be interesting new spectroscopic techniques also in biophysical spectroscopy.

The advances in application of SERS in biophysics during the recent half decade promise a bright future for this scientific field, which combines modern laser spectroscopy and nanotechnology. A comprehensive, quantitative understanding of the mechanisms of SERS, which should be achieved during the next few years, might be an important key for further development of SERS as a tool in biomedical spectroscopy. Considerable steps ahead are also expected in developing new 'SERS-active' nanostructures for specific applications in life sciences and biophysics, tailored and optimized using new nanotechnologies [99].

References

[1] Fleischman M, Hendra P J and McQuillan A J 1974 *Chem. Phys. Lett* **26** 123
[2] Jeanmaire D L and Duyne R P V 1977 *J. Electroanal. Chem.* **84** 1
[3] Albrecht M G and Creighton J A 1977 *J. Am. Chem. Soc.* **99** 5215

[4] Seki H J 1986 *J. Electron Spectrosc. Relat. Phenom.* **39** 239
[5] Otto A 1984 Surface-enhanced Raman scattering: 'classical' and 'chemical' origins *Light Scattering in Solids IV. Electronic Scattering, Spin Effects, SERS and Morphic Effects* ed M Cardona and G Guntherodt (Berlin: Springer) p 289
[6] Moskovits M 1985 *Rev. Mod. Phys.* **57** 783
[7] Bachackashvilli A, Efrima S, Katz B and Priel Z 1983 *Chem. Phys. Lett.* **94** 571
[8] Kneipp K, Hinzmann G and Fassler D 1983 *Chem. Phys. Lett.* **99** 5
[9] Hildebrandt P and Stockburger M 1984 *J. Phys. Chem.* **88** 5935
[10] Pettinger B 1984 *Chem. Phys. Lett.* **110** 576
[11] Kneipp K, Kneipp H and Rentsch M 1987 *J. Mol. Struct.* **156** 3
[12] Pettinger B and Krischer K 1987 *J. Electron Spectrosc. Relat. Phenom.* **45** 133
[13] Kneipp K 1988 *Exp. Tech. Phys.* **36** 161
[14] Kneipp K, Wang Y, Kneipp H, Itzkan I, Dasari R R and Feld M S 1996 *Phys. Rev. Lett.* **76** 2444
[15] Kneipp K, Wang Y, Kneipp H, Perelman L T, Itzkan I, Dasari R R and Feld M S 1997 *Phys. Rev. Lett.* **78** 1667
[16] Nie S and Emory S R 1997 *Science* **275** 1102
[17] Kneipp K, Kneipp H, Deinum G, Itzkan I, Dasari R R and Feld M S 1998 *Appl. Spectrosc.* **52** 175
[18] Kneipp K, Kneipp H, Kartha V B, Manoharan R, Deinum G, Itzkan I, Dasari R R and Feld M S 1998 *Phys. Rev.* E **57** R6281
[19] Kneipp K, Kneipp H, Itzkan I, Dasari R R and Feld M S 1999 *Chem. Rev.* **99** 2957
[20] Xu H X, Bjerneld E J, Kall M and Borjesson L 1999 *Phys. Rev. Lett.* **83** 4357
[21] Michaels A M, Nirmal M and Brus L E 1999 *J. Am. Chem. Soc.* **121** 9932
[22] Bjerneld E J, Johansson P and Käll M 2000 *Single Mol.* **1** 239
[23] Constantino C J L, Lemma T, Antunes P A and Aroca R 2001 *Anal. Chem.* **73** 3674
[24] Wessel J 1985 *J. Opt. Soc. Am.* B **2** 1538
[25] Shalaev V M 1996 *Phys. Rep.* **272** 61
[26] Safanov V P, Shalaev V M, Markel V A, Danilova Y E, Lepeshkin N N, Kim W, Rautian S G and Armstrong R L 1998 *Phys. Rev. Lett.* **80** 1102
[27] Kneipp K *et al* 2000 *Phys. Rev. Lett.* **84** 3470
[28] Marlin J C 1985 *Pure Appl. Chem.* **57** 785
[29] Thomas L L, Kim J H and Cotton T M 1990 *J. Am. Chem. Soc.* **112** 9378
[30] Lutz M (ed) 1991 *Chlorophylls* (Boca Raton, FL: Chemical Rubber Company)
[31] Seibert M, Picorel R, Kim J H and Cotton T M 1992 *Methods Enzymol.* **213** 31
[32] Lutz M 1995 *Biospectroscopy* **1** 313
[33] Picorel R, Chumanov G, Torrado E, Cotton T M and Seibert M 1998 *J. Phys. Chem.* B **102** 2609
[34] Niki K, Kawasaki Y, Kimura Y, Higuchi Y and Yasuoka N 1987 *Langmuir* **3** 982
[35] Murgida D H and Hildebrandt P 2001 *J. Am. Chem. Soc.* **123** 4062
[36] Cotton T M 1985 *Surface and Interfacial Aspects of Biomedical Polymers* ed J Andrade (New York: Plenum) p 161
[37] Koglin E and Sequaris J M 1986 *Top. Curr. Chem.* **134** 1
[38] Cotton T M 1988 *Spectroscopy of Surfaces* ed R J H Clark and R E Hester (New York: Wiley) p 91
[39] Paisley R F and Morris M D 1988 *Prog. Anal. Spectrosc.* **11** 111
[40] Cotton T M, Kim Jae-Ho and Chumanov G D 1991 *J. Raman Spectrosc.* **22** 729
[41] Sokolov K, Khodorchenko P, Petukhov A, Nabiev I, Chumanov G and Cotton T M 1993 *Appl. Spectrosc.* **47** 515
[42] Ferraro J R 1994 *Introductory Raman Spectroscopy* (New York: Academic)
[43] Schrader B (ed) 1995 *Infrared and Raman Spectroscopy: Methods and Applications* (Chichester: Wiley)
[44] Moskovits M 1978 *J. Chem. Phys.* **69** 1459
[45] Kerker M, Siiman O, Bumm L A and Wang D S 1980 *Appl. Opt.* **19** 3253
[46] Wang D S and Kerker M 1981 *Phys. Rev.* B **24** 1777
[47] Zeman E J and Schatz G C 1987 *J. Phys. Chem.* **91** 634
[48] Xu H X, Aizpurua J, Kall M and Apell P 2000 *Phys. Rev.* E **62** 4318
[49] Inoue M and Ohtaka K 1983 *J. Phys. Soc. Japan* **52** 3853
[50] Weitz D A and Oliveria M 1984 *Phys. Rev. Lett.* **52** 1433
[51] Stockman M I, Shalaev V M, Moskovits M, Botet R and George T F 1992 *Phys. Rev.* B **46** 2821
[52] Yamaguchi Y, Weldon M K and Morris M D 1999 *Appl. Spectrosc.* **53** 127
[53] Poliakov E Y, Shalaev V M, Markel V A and Botet R 1996 *Opt. Lett.* **21** 1628
[54] Shalaev V M, Botet R, Mercer J and Stechel E B 1996 *Phys. Rev.* B **54** 8235
[55] Gadenne P, Brouers E, Shalaev V M and Sarychev A K 1998 *J. Opt. Soc. Am.* B **15** 68

[56] Sarychev A K and Shalaev V M 2000 *Phys. Rep.* **335** 275
[57] Podolskiy V A and Shalaev V M 2001 *Laser Phys.* **11** 26
[58] Markel V A, Shalaev V M, Zhang P, Huynh W, Tay L, Haslett T L and Moskovits M 1999 *Phys. Rev.* B **59** 10 903
[59] Gadenne P, Quelin X, Ducourtieux S, Gresillon S, Aigouy L, Rivoal J C, Shalaev V and Sarychev A 2000 *Physica* B **279** 52
[60] Gresillon S, Rivoal J C, Gadenne P, Quelin X, Shalaev V and Sarychev A 1999 *Phys. Status Solidi* a **175** 337
[61] Kneipp K, Kneipp H, Itzkan I, Dasari R R and Feld M S 1999 *Chem. Phys.* **247** 155
[62] Kneipp K, Kneipp H, Itzkan I, Dasari R R and Feld M S 2000 Scanning and force microscopies for biomedical applications II *Proc. SPIE* **3922** 49
[63] Otto A, Mrozek I, Grabhorn H and Akemann W 1992 *J. Phys.: Condens. Matter* **4** 1143
[64] Campion A and Kambhampati P 1998 *Chem. Soc. Rev.* **27** 241
[65] Jiang J D, Burstein E and Kobayashi H 1986 *Phys. Rev. Lett.* **57** 1793
[66] Arenas J F, Woolley M S, Tocon I L, Otero J C and Marcos J I 2000 *J. Chem. Phys.* **112** 7669
[67] Persson B N J 1981 *Chem. Phys. Lett.* **82** 561
[68] Otto A 2001 *Phys. Status Solidi* **188** 1455
[69] Kambhampati P, Child C M, Foster M C and Campion A 1998 *J. Chem. Phys.* **108** 5013
[70] Sass J K, Neff H, Moskovits M and Holloway S 1981 *J. Phys. Chem.* **85** 621
[71] Ayars E J, Hallen H D and Jahncke C L 2000 *Phys. Rev. Lett.* **85** 4180
[72] Ayars E J, Jahncke C L, Paesler M A and Hallen H D 2001 *J. Microsc.—Oxford* **202** 142
[73] Kneipp K, Jorio A, Kneipp H, Brown S D M, Shafer K, Motz J, Saito R, Dresselhaus G and Dresselhaus M S 2001 *Phys. Rev.* B **6308** 1401
[74] Creighton J A, Blatchford C G and Albrecht M G 1979 *J. Chem. Soc. Faraday Trans.* II **75** 790
[75] Lee P C and Meisel D 1982 *J. Phys. Chem.* **86** 3391
[76] Fojtik A and Henglein A 1993 *Ber. Bunsenges. Phys. Chem.* **97** 252
[77] Nedderson J, Chumanov G and Cotton T M 1993 *Appl. Spectrosc.* **47** 1959
[78] Kneipp K, Wang Y, Dasari R R and Feld M S 1995 *Appl. Spectrosc.* **49** 780
[79] Kneipp K and Kneipp H 1993 *Spectrochim. Acta* A **49** 167
[80] Kneipp K 1994 *Spectrochim. Acta* A **50** 1023
[81] Wang X, Wen H, He T J, Zuo J, Xu C Y and Liu F C 1997 *Spectrochim. Acta* A **53** 2495
[82] Szabo N J and Winefordner J D 1997 *Appl. Spectrosc.* **51** 965
[83] Lyon L A, Keating C D, Fox A P, Baker B E, He L, Nicewarner S R, Mulvaney S P and Natan M J 1998 *Anal. Chem.* **70** 341R
[84] Kneipp K, Jahr W and Roewer G 1989 *Chem. Phys. Lett.* **163** 105
[85] Kneipp K 1990 *J. Mol. Struct.* **218** 357
[86] Gliemann H, Nickel U and Schneider S 1998 *J. Raman Spectrosc.* **29** 1041
[87] Stokes D L and Vo-Dinh T 2000 *Sensors Actuators* B **69** 28
[88] Viets C and Hill W 2000 *J. Raman Spectrosc.* **31** 625
[89] Todd A E and Morris M D 1993 *Appl. Spectrosc.* **47** 855
[90] Weldon M K, Zhelyaskov V R and Morris M D 1998 *Appl. Spectrosc.* **52** 265
[91] Buchel D, Mihalcea C, Fukaya T, Atoda N, Tominaga J, Kikukawa T and Fuji H 2001 *Appl. Phys. Lett.* **79** 620
[92] Mihalcea C, Buchel D, Atoda N and Tominaga J 2001 *J. Am. Chem. Soc.* **123** 7172
[93] Anderson M S 2000 *Appl. Phys. Lett.* **76** 3130
[94] Stockle R M, Yung Doug S, Deckert V and Zenobi R 2000 *Chem. Phys. Lett.* **318** 131
[95] Pettinger B, Picardi G, Schuster R and Ertl G 2000 *Electrochemistry* **68** 942
[96] Hayazawa N, Inouye Y, Sekkat Z and Kawata S 2000 *Opt. Commun.* **183** 333
[97] Hayazawa N, Inouye Y, Sekkat Z and Kawata S 2001 *Chem. Phys. Lett.* **335** 369
[98] Nieman L T, Krampert G M and Martinez R E 2001 *Rev. Sci. Instrum.* **72** 1691
[99] Jensen T R, Malinsky M D, Haynes C L and Van Duyne R P 2000 *J. Phys. Chem.* B **104** 10 549
[100] Hillenbrand R and Keilmann F 2001 *Appl. Phys.* B **73** 239
[101] Kneipp K, Kneipp H, Manoharan R, Hanlon E B, Itzkan I, Dasari R R and Feld M S 1998 *Appl. Spectrosc.* **52** 1493
[102] So P T C, Dong C Y, Masters B R and Berland K M 2000 *Annu. Rev. Biomed. Eng.* **2** 399
[103] Zumbusch A, Holtom G R and Xie X S 1999 *Phys. Rev. Lett.* **82** 4142
[104] Volkmer A, Cheng J X, Book L D and Xie X S 2001 *Biophys. J.* **80** 656.29
[105] Cheng J X, Volkmer A, Book L D and Xie X S 2001 *J. Phys. Chem.* B **105** 1277
[106] Volmer A, Cheng J X and Xie X S 2001 *Phys. Rev. Lett.* **87** 23 901
[107] Mertz J, Xu C and Webb W W 1995 *Opt. Lett.* **20** 2532

[108] Xu H, Bjerneld E J, Kåll M and Borjesson L 1999 personal communication
[109] Garrell R L, Herne T M, Ahern A M and Sullenberger E 1990 Optical fibers in medicine V *Proc. SPIE* **1201** 451
[110] Nabiev I R, Sokolov K V and Manfait M (ed) 1993 *Biomolecular Spectroscopy* (Chichester: Wiley)
[111] Ruperez A, Montes R and Laserna J J 1991 *Vib. Spectrosc.* **2** 145
[112] Nabiev I R, Morjani H and Manfait M 1991 *Eur. Biophys. J.* **19** 311
[113] Barton T F, Cooney R P and Denny W A 1992 *J. Raman Spectrosc.* **23** 341
[114] Morjani H, Riou J F, Nabiev I, Lavelle F and Manfait M 1993 *Cancer Res.* **53** 4784
[115] Nabiev I, Chourpa I and Manfait M 1994 *J. Phys. Chem.* **98** 1344
[116] Nabiev I, Baranov A, Chourpa I, Beljebbar A, Sockalingum G D and Manfait M 1995 *J. Phys. Chem.* **99** 1608
[117] Wood E, Sutton C, Beezer A E, Creighton J A, Davis A F and Mitchell J C 1997 *Int. J. Pharmaceutics* **154** 115
[118] Westerink B H, Damsma G, Rollema H, de Vries J D and Horn A S 1987 *Life Sci.* **41** 1763
[119] Schulze H G, Blades M W, Bree A V, Gorzalka B G, Greek L S and Turner R B 1994 *Appl. Spectrosc.* **48** 50
[120] Lee N S, Hsieh Y Z, Paisley R F and Morris M D 1988 *Anal. Chem.* **64** 442
[121] McGlashen M L, Guhathakurta U and Davis K L 1991 *Appl. Spectrosc.* **45** 543
[122] Morris M D, McGlashen M L and Davis K L 1990 Optical fibers in medicine V *Proc. SPIE* **1201** 447
[123] Kneipp K, Wang Y, Dasari R R and Feld M S 1995 *Spectrochim. Acta* A **51** A 481
[124] O′Neal D P, Motamedi M, Chen J and Cote G L 2000 Biomedical spectroscopy: vibrational spectroscopy and other novel techniques *Proc. SPIE* **3918** 191
[125] Shear J B and Gostkowski M L 1998 *J. Am. Chem. Soc.* **120** 12 966
[126] Naumann D, Helm D and Labischinski H 1991 *Nature* **351** 81
[127] Chadha S, Nelson W H and Sperry J F 1993 *Rev. Sci. Instrum.* **64** 3088
[128] Efrima S and Bronk B V 1998 *J. Phys. Chem.* B **102** 5947
[129] Sockalingum G D, Lamfarraj H, Beljebbar A, Pina P, Delavenne M, Witthun F, Allouch P and Manfait M 1999 Biomedical applications of Raman spectroscopy *Proc. SPIE* **3608** 185
[130] Rohr T E, Cotton T, Fan N and Tarcha P J 1989 *Anal. Biochem.* **182** 388
[131] Ni J, Lipert R J, Dawson G B and Porter M D 1999 *Anal. Chem.* **71** 4903
[132] Dou X, Takama T, Yamaguchi Y, Yamamoto H and Ozaka Y 1997 *Anal. Chem.* **69** 1492
[133] Hawi S R, Rochanakij S, Adar F, Campbell W B and Nithipatikom K 1998 *Anal. Biochem.* **259** 212
[134] Dou X, Takama T, Yamaguchi Y, Hirai K, Yamamoto H, Doi S and Ozaki Y 1998 *Appl. Opt.* **37** 759
[135] Richterich P and Church G M 1993 *Methods Enzymol.* **218** 187
[136] Nirmal M, Dabbousi B O, Bawendi M G, Macklin J J, Trautman J K, Harris T D and Brus L E 1996 *Nature* **383** 802
[137] Han M Y, Gao X H, Su J Z and Nie S 2001 *Nature Biotechnol.* **19** 631
[138] Vo-Dinh T, Stokes D L, Griffin G D, Volkan M, Kim U J and Simon M I 1999 *J. Raman Spectrosc.* **30** 785
[139] Vo-Dinh T, Houck K and Stokes D L 1994 *Anal. Chem.* **66** 3379
[140] Isola N R, Stokes D L and Vo-Dinh T 1998 *Anal. Chem.* **70** 1352
[141] Graham D, Mallinder B J and Smith W E 2000 *Biopolymers* **57** 85
[142] Koglin E, Sequaris J M and Valenta P 1981 *Z. Naturf.* **360** 809
[143] Kneipp K and Flemming J 1986 *J. Mol. Struct.* **145** 173
[144] Nabiev I R, Sokolov K V and Voloshin O N 1990 *J. Raman Spectrosc.* **21** 333
[145] Kneipp K, Pohle W and Fabian H 1991 *J. Mol. Struct.* **244** 183
[146] Chumanov G and Cotton T M 1999 Biomedical applications of Raman spectroscopy *Proc. SPIE* **3608** 204
[147] Keller R 1990 *Los Alamos Annual Report*
[148] Thornton J and Force R K 1991 *Appl. Spectrosc.* **45** 1522
[149] Sheng R, Nii F and Cotton T M 1991 *Anal. Chem.* **63** 437
[150] Beljebbar A, Sockalingum G D, Morjani H and Manfait M 1999 Biomedical applications of Raman spectroscopy *Proc. SPIE* **3608** 175
[151] Kneipp K, Haka A S, Kneipp H, Badizadegan K, Yoshizawa N, Boone C, Shafer-Peltier K E, Motz J T, Dasari R R and Feld M S 2002 *Appl. Spectrosc.* **56** 150
[152] Puppels G J, Mul F F M D, Otto C, Greve J, RobertNicoud M, Arndt-Jovin D J and Jovin T 1990 *Nature* **347** 301
[153] Otto C, de Grauw C J, Duindam J J, Sijtsema N M and Greve J 1997 *J. Raman Spectrosc.* **28** 143
[154] Weitz D A, Garoff S, Gersten J I and Nitzan A 1983 *J. Chem. Phys.* **78** 5324
[155] Sokolov K, Chumanov G and Cotton T M 1998 *Appl. Chem.* **70** 3898
[156] Constantino C J L and Aroca R F 2000 *J. Raman Spectrosc.* **31** 887